Prevention of Track Buckling and Rail Fracture by Non-destructive Testing of the Neutral Temperature in cw-Rails

Dr. Alfred Wegner, Goldschmidt-Thermit Group, Elektro-Thermit GmbH & Co.KG, Chemiestrasse 24, D-06132 Halle/Saale, Germany, Tel. +49-345-7795-802

Summary: Continuously welded rails generate forces, which can cause dangerous rail failures, if not managed. A recently developed method allows the fast non-destructive (nd) determination of rail stresses, weakened track conditions and neutral temperature in fixed track between traffic. Based on the magneto-elastic principle the interaction with the microstructure is measured. The amplitude of the detected Magnetic Barkhausen Noise (MBN) containing the pulses generated in the rail depends on the stress. The latter may become complex in curves and under weakened track conditions, which requires special attention. The presented technique offers a wide spread use for neutral temperature measurements and covers the actual need of a non-destructive SFT measuring technique.

Index Therms: Neutral Temperature, Longitudinal Force, Track Security

1. Introduction

Due to the increasing demands on the quality of continuously welded (cw) rails, non-destructive testing technologies become more and more important. In the rails used in the construction of cw track structures lower or higher residual stresses are present due to processes of manufacturing. Further mechanical stresses are added to these residual stresses by dead weight and installation. The task of determining the longitudinal stresses acting in a rail of cw railway track is not a simple technical problem. The application of destructive test methods is not expedient, because in the case of a railway track such tests require the separation of the cw-rail or its unfastening and moving and thus the eventual modification of stresses.

In a welded track the sleepers prevent displacement of rails through the track fastening elements. After the rails have been clamped, any temperature change causes a thermal stress in the rails due to restriction of dilatation. The temperature at which the thermal stress in the tested cross section of a rail is zero is defined as neutral or stress free temperature. It is important that the neutral temperature be in the vicinity of the average of expectable highest and lowest rail temperatures. Should the discrepancy from that average be large, at low temperatures rail ruptures, at high temperatures rail buckling may occur. By the help of an appropriate non-destructive testing technology the magnetic measurement of the neutral temperature at cw rails in fixed track between traffic is possible. The measuring device operates by means of non-contact gauging using the magneto-elastic principle and allows fast measurement and documentation of actual neutral temperature of most rail types. The longitudinal stress and the Neutral Temperature are determined by measurement of characteristic magnetic values.

2. Problem definition - Inspection demand

The system wheel – rail consists of individual system components, where the vehicle components are well known. Their behaviour can be described by mathematically. The superstructure, however, can not be described by an exact analysis. Consequently its description is mainly achieved by experiences based on relationships and parameters derived from empirical tests. The neutral temperature defines the relation of the rail stress distribution and is thus a key magnitude. Primary important parameters like the security against fracture and buckling but also the driving comfort depend decisively of the neutral temperature. Therefore the judgment of the security against geometrical alterations of the cw-rail, is indispensable. Because the proximate cause for geometrical changes is the result of the action of forces, it is important to determine the track security including the forces. For this inspection a non-destructive measuring technique is required.

3. Physical backgrounds

Every part of ferromagnetic materials contributes to the magnetization. The internal magnetization, however, is not uniform down to the microscopic scale. Many magnetic domains are magnetized in a different direction. The magnetization inside each domain is made up of many atomic moments which are lined up by the action of their exchange force /1/. This explains why ferrous materials have a domain structure. The crystallites are limited by grain boundaries, the magnetic domains by the Bloch-walls. In 1932, Bloch described that the boundary between the domains is not sharp on an atomic scale but is spread over a certain thickness wherein the direction of spins changes gradually. Two kinds of Bloch-walls have to be defined: The 90°-(BW1) and the 180°-Bloch-wall (BW2). It is important to add that these different wall types interact in a different way with the magnetic field during the magnetization. They exhibit a fairly complex change in magnetization upon the application of a magnetic field. This behaviour can be described by a magnetization curve possessing three distinct regions I, II and III (fig. 1). Starting from a demagnetized state, the magnetization increases (broken curve) and finally reaches the saturation magnetization. In the region “I” the process of magnetization is almost reversible. Beyond this region the processes of magnetization are no longer reversible. BW2 do not interact with macro and micro stresses /2/. Beside BW1 all rotation processes RP are stress sensitive.

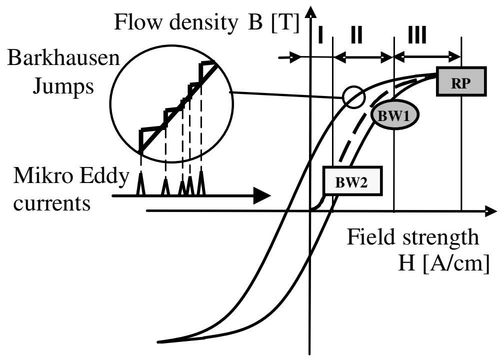

Fig. 1: Magnetization regions and field dependent magnetization processes.

Hereby stresses are measured by values mainly determined by BW1. During this process, micro eddy currents are induced in the volume (Fig. 1). These so-called Barkhausen jumps can be measured by an appropriate detector. The effective value of MBN is recognized as a measure for quantitative evaluations.

If a longitudinal load stress is applied, the permeability for the applied magnetic field changes. Tension leads to an increase of the permeability. The higher the longitudinal stress, the higher the increase of permeability. The rail becomes more and more easily magnetizable. The opposite case appears, when compression stress is applied. With increasing compression the rail becomes magnetic hard. The permeability for the magnetic field decreases. The MBN contains the eddy currents of the stress sensitive processes /3, 4/. Reading the MBN for different load stresses a calibration on longitudinal load stress is received (fig. 5).

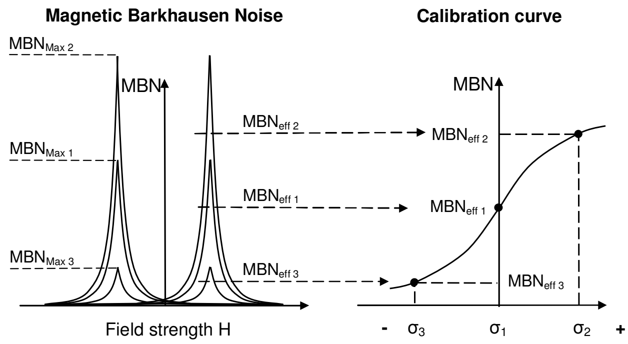

Fig.2: Calibration of MBN on load stress.

4. FUNCTIONAL PRINCIPLE

For producing the MBN, the rail is energized in the direction perpendicular to the measured cross-sectional area and the magnetic Barkhausen noise emitted from the surface is measured at the tested cross-section. The MBN is measured at the surface with a sensor containing a ferromagnetic material and matched to the given cross-sectional area. Imperfect matching due to unevenness of surface, scale, rust, contamination or paint coating reduces the magnitude of the detected MBN. In order to eliminate inaccuracies resulting from such locations, the spacing between the ferromagnetic material and the investigated surface, the so-called air gap, is measured, and the magnitude of the detected MBN is corrected according to the measured depth of the air gap.

5. DEVICE AND OPERATION METHOD

One measurement consists of 50 readings distributed along a length of typically 60 meters, other base lengths are possible on request. The non contacting measurement is performed after positioning the device above each point in turn. The readings are stored in the measuring computer. Fig. 3A shows the manually operated railcar on with the central unit and the measuring probe (fig. 3B) are placed. The probe consists of two yokes that are pressed around the rail head and temperature sensors.

A

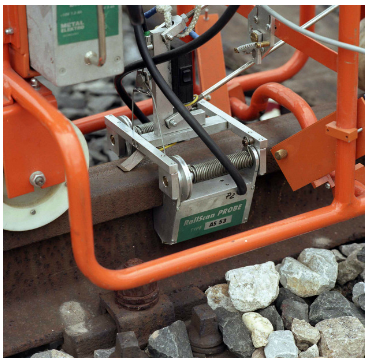

B

Fig. 3: Measuring device in use. A: Operator and device, B: Probe, coupled to the rail head.

6. EVALUATION

After completing the measurements the raw data are exported to PC and stored for further evaluation. The evaluation is performed via software evaluation tools. The result is achieved via evaluating and plotting the measuring values of the magnetic parameter ß and rail temperature versus the longitudinal coordinate and measuring point number (fig.4) and furthermore depicting the load stress determined by means of the averaged magnetic parameters and the calibration curve (fig. 5). The neutral temperature is calculated by means of equation (1), with the load stress σ, the elasticity modulus E, the thermal expansion coefficient α and the rail temperature T_{Rail}.

$$T_N = \frac{\sigma}{E \times \alpha} + T_{Rail} \tag{1}$$

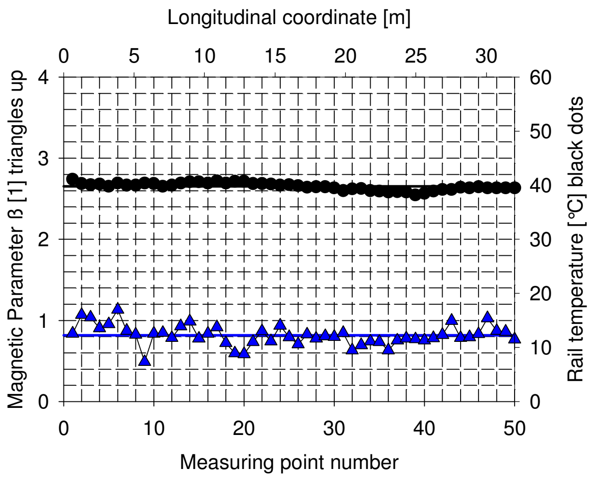

Fig. 4: Stress sensitive parameter and rail temperature, plotted vs. longitudinal coordinate.

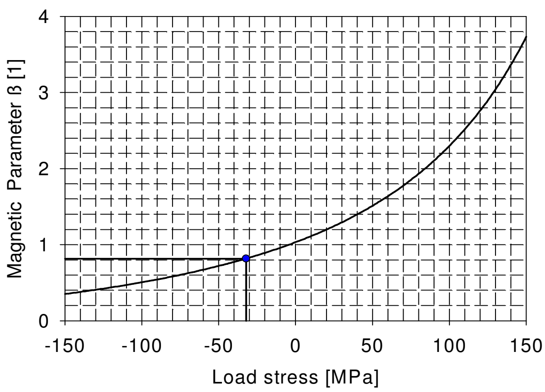

Fig. 5: Longitudinal load stress determined by means of the rail specific calibration curve.

7. RESULT AND DOCUMENTATION

The results of the inspected locations are summarized in a report containing all track relevant information, i.e. the measured neutral temperatures linked to their location and position in the cw-rail. Fig. 6 is an example for a visual plot of the measured areas.

8. FINDINGS IN THE CW-RAIL BY ND-SFT INSPECTION TECHNIQUE

Enabling fast non-destructive measurements at cw-rails multiple experiences about the superstructure behaviour become possible. In the following some essential findings and the potential for optimizing maintenance strategies are presented.

8.1. Behaviour of curves

The selected track in fig. 6 shows a curve located between two long straight areas. The required neutral temperature is 38°C. Therefore the neutral temperature values of smaller than 30°C in the transitions to the curve are significantly to low whereas the values taken near the curve apex are still high enough. Following previous work /5/ this result depicts a typical behaviour of curves owning a decreased ballast resistance. Obviously the forces introduced from the straight areas acting in the transitions to the curve lead to an increase of compression and therefore to a decreased neutral temperature. With regard to their large radius and small length it is obvious that the transitions behave more like straights than like curves. The forces in the transition can be considered as a superposition of the thermal force and the forces due to permanent strains eventually caused by longitudinal creep effects. In the curve itself these forces lead to a lateral displacement of the rails attached on the sleepers. Evidently this arises due to the decreased lateral ballast resistance. The lateral movement itself results in a decrease of the longitudinal force and stress and therefore to an increase of the neutral temperature. Considering the neutral temperature as a measure for the track quality and its security against buckling and fracture such a measuring result in curve apex may result in the dangerous misinterpretation that the stress state in the cw-rail is correct. The possible consequence that such curves are not maintained or stressed until further notice has to be avoided. The position safety and therefore the safety against bucking are no more given at all in such a section. Such cases may eventually be one reason for arising difficulties regarding succeeded safety risk prevention.

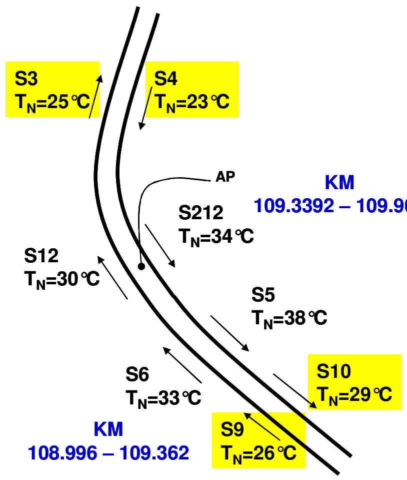

Fig. 6: Visual depiction of the measuring result given in table 1.

The experiences resulting of the use of the presented non-destructive neutral temperature measuring technique underline that the actual state-of-the-art in longitudinal force management makes necessary the possibility of an easy, fast and particularly non-destructive local neutral temperature measurement technique.

8.2. Judgement of maintenance techniques

The problem of recognizing critical track areas like described above can only be solved by a detailed and experimentally verified knowledge of the superstructure to be maintenanced. Considering the example of fig. 6 it was found that the neutral temperature changes during the thermal cycles. Obviously there exist two extreme values: A maximum if the rail temperature is high and a minimum if it is low, what corresponds to the predictions given in /6/.

This result means that such critical areas can only be detected in the tension range of the rail.

Collecting more and more SFT results several further important experiences were made. Considering the example of critical areas to be restressed it was recognized by means of the results that under certain conditions it becomes impossible to maintain a location by simple stressing action without renewing or maintaining the superstructure including the components, i.e. the ballast. With regard to the stressing procedures there are three main methods to perform neutralization: 1. by introducing artificial heat, 2. by solar heating and 3. by means of a hydraulic tensor. In this context it is important to know that only method 1 enables a correct neutralization. Both other methods can lead to a longitudinal movement of the fastened areas /6/ what could result in an incorrect neutralization, particularly in critical areas where the ballast resistance is reduced. Typically it happens that the elongation of the rail during tensioning is distributed along a different, greater rail length and consequently the introduced strain amplitude is not sufficiently high to ensure the desired stress and neutral temperature. In the case of a particular decreased ballast resistance this means that a track can no more be stressed by simple neutralization because the required stress level can not be introduced into the rail. A particular large error arises if the critical location is restressed by solar heating or hydraulic tensioning using conventional adjustment tables that are strictly speaking only valid for artificial heating /6/. In order to substantiate such predictions Elektro-Thermit performed tests like shown in fig. 7. A special set-up allowing displacement measurement was worked out at a location possessing a low neutral temperature: In a curve transition to a 1400m radius and a length of approx. 900m RailScan measurements were recorded and evaluated. Hereafter longitudinal displacement measurements were enabled placing two lasers and two wires in the height of the characteristic areas. The lasers were placed at the ends of the rail length to be unfastened, the wires 20m deep away in the fastened areas. Then the cw-rail was separated by rail cut, the rail temperature was measured and the neutral temperature calculated by equation (2) or appropriate adjustment tables.

$$T_N = \frac{\varepsilon}{\alpha} + T_{Rail} = \frac{\Delta l}{\alpha \times l} + T_{Rail} \qquad (2)$$

where ε is the longitudinal strain, Δl is the longitudinal displacement (here the cut length was taken) and l the unfastened length. For a rail temperature of 14 °C, a base length of 122 m taken from the adjustment table and a measured gape size of 40 mm the calculation lead to a neutral temperature of 43 °C. The comparison of this value with the nd- measurement leads to a difference of 10 °C. A similar different result is obtained comparing the measured gap size with the expected gape size determined by means of nd- value by means of equation (3).

$$\Delta l = \alpha \times l \times (T_{NRailScan} - T_{Rail}) \qquad (3)$$

The reason for the difference can be found in the measuring result of the longitudinal displacement. Fig. 7 shows that approx. 7 mm displacement deriving from outside the fastened area are not considered in the chosen base length of 122m. The calculation of a corrected base length lead to a value of approx. 160 m. This results in a neutral temperature of 35 °C what corresponds to the non-destructive result (see also chapters 8.3 and 8.4). This example clearly shows that adjustment tables have to be verified continuously in order to avoid errors.

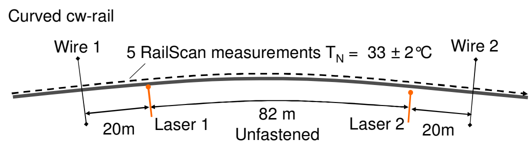

	1	2	Displacement measurement	3	4
	Wire 1	Laser 1	Gap after cut and relaxation	Laser 2	Wire 2
U	2-3	15	40 (both directions)	9.5	4

U – Longitudinal displacement [mm]

Fig. 7: Comparison measurement non-destructive – destructive and verification of anchor movement by displacement measurement

8.3. Stress state and distribution in curves

In curves the stress distribution due to bending stresses has to be taken into account evaluating the RailScan measurements. Fig. 8 shows the main stress effects that occur: In a straight and well aligned cw-rail there are acting only longitudinal stresses caused by thermal effects (Fig. 8A). In a curve bending stresses are added to the thermal stress (Fig. 8B). If a lateral displacement of the curve is possible further bending stresses are added (Fig. 8C). The amplitude of these bending stresses known as curve breathing is usually small and neglecteable for long curves possessing a large radius. Therefore the effect is usually neglectable also for RailScan measurements. Considering straight bending of the curve the bending stress is symmetrical to the vertical axis of the rail.

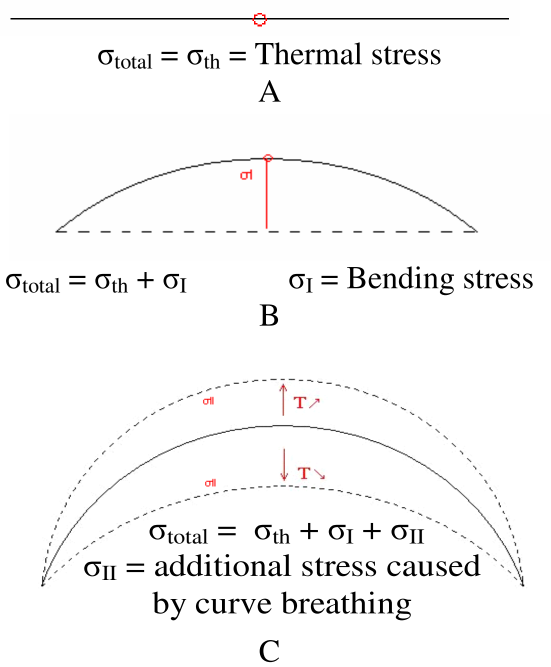

Fig. 8: A: Straight section without any misalignment- The total stress corresponds to the uniform longitudinal thermal stress, B: Curve without misalignment and high ballast resistance- The total stress consists of the thermal stress and the bending stress, C: Curve without misalignment and reduced ballast resistance- the total stress is supplemented by the bending stress caused by the curve breathing

In some special cases the effects of bending is no more neglectable. Because the lateral force in a curve is introduced by means of the fastening system in the rail foot the rail bending is in fact not straight. Because the load plane does not lead through the emphasis the neutral axis is more or less shifted. The bending is crooked. Fig. 9 shows such a bended rail i.e. in a curve. The stresses plotted in the figure were calculated for the rail head because the nd-measuring technique presented in this article catches the stresses in this zone of the rail.

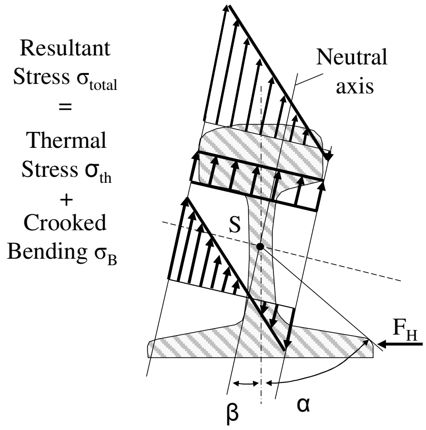

Fig. 9: Longitudinal stress and its crossectional distribution in a bended cw-rail

The crooked bending leads to an asymmetrical bending stress distribution, where the stresses on the drawn surface are increased and the compression stresses on the opposite side are decreased. This effect is further increased in used rails with reduced height of the rail head.

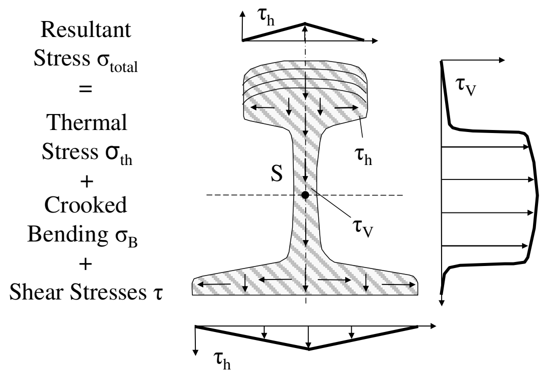

Fig. 10: Horizontal and vertical shear stresses caused by horizontal rail bending of the rail shown in fig. 8B and fig. 9

The rail bending i.e. in curves causes a further stress component that needs attention. The rail possesses a cross section similar to this of a girder. In proportion to their height the thickness of web, foot and head is relatively small. Consequently horizontal, vertical and longitudinal shear stresses appear in the rail and are added to the normal stresses shown in fig. 9. Consequently the stress state of bended rails becomes multi axial. The different stress components therefore have to be considered evaluating the nd-results following their nature and their interaction with the non-destructive technique.

Normal stresses like caused by temperature changes or bending produce volume changes in the rail. Shear stresses create changes of the rail shape. The combined effect of these stresses can be depicted by the corresponding required energy. In previous work Von Mises proposed the introduction of an equivalent stress σ_V for the treatment of complex stress states /2/. This stress is derived from the required energy. The expression, simplified for the case of a curved cw-rail has then the form:

$$\sigma_V = \sqrt{\sigma^2 + 3 \times \tau^2} \qquad (4)$$

where σ is the total longitudinal normal stress and τ is the sum of the shear stresses.

8.4. Measurements in misaligned locations

Investigating the stress state of bended rails one result of the previous chapters was that in long curves of large radius the bending stress is neglectable. For short curves, small radius and thus for misalignments this stress component has to be examined closely. The bending stress can be calculated by means of equation (5).

$$\sigma_{border} = \frac{E}{\rho} \times \frac{h}{2} \qquad (5)$$

with the elasticity modulus $E = 2.1 \text{x} 10^5$ MPa, ρ the curvature and h the width of the rail head. Because misalignments typically are noticed with regard to their amplitude and length the required radius in equation (5) has to be calculated by the help of equation (6).

$$R = \frac{a}{2} + \frac{L^2}{8a} \qquad (6)$$

where R is the radius, a the misalignment amplitude and L its base length. Fig. 11 shows a typical misalignment in a curve and the calculated stress plotted vs. different alignment errors and base lengths. It is obvious that the bending stress increases significantly with increasing misalignment error sizes and decreasing base lengths. It is important to understand this appearance with regard to the consequence on the longitudinal force acting in the rail: The stress increase alone doesn't explain the eventual danger of track stability. It is the excentrical impact of the resulting longitudinal force leading under critical conditions to the sudden deflection of the track. With the presented nd-technique the diagnostic of these special cases become possible.

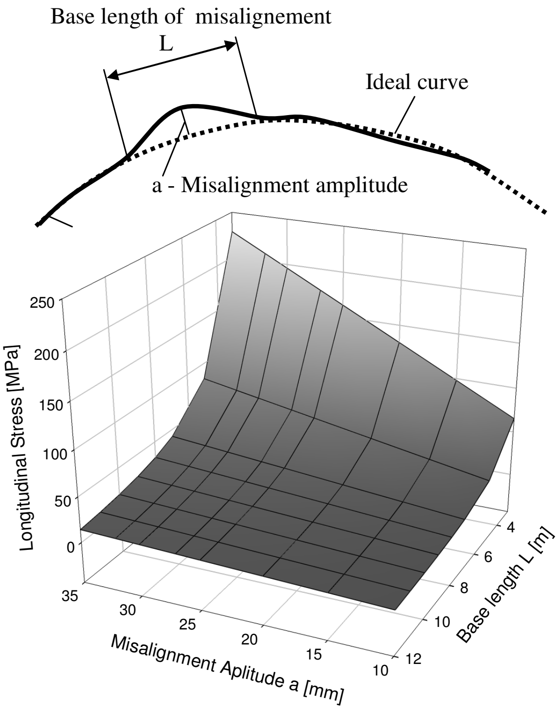

Fig. 11: Depiction of an alignment error situated in a curve and resulting bending stress

9. CALIBRATION

Before measurement the device is calibrated in the laboratory using calibration rails. On this occasion, measurements of the MBN are taken for different longitudinal stresses and used for plotting a calibration curve of the MBN as a function of longitudinal stress. Fig. 12 shows a typical calibration test stand.

Before performing the calibration, the excitation of the magnetic field has to be defined. Therefore each rail type has to be magnetized individually in order to set the optimal excitation amplitude. After the excitation parameters are defined, the calibration measurement is performed. Hereby several well defined longitudinal stress levels are applied. The device is positioned and the probe is coupled to the rail head. During the magnetization of the rail the MBN is measured. After the measurement of the rail temperature the signals are evaluated and the characteristic values ß are determined. Finally a calibration curve is plotted (fig. 5). Hereafter the neutral temperature can be determined easily by nd-measurement at cw-rails and calculation using the modulus of elasticity, the coefficient of thermal expansion and the rail temperature.

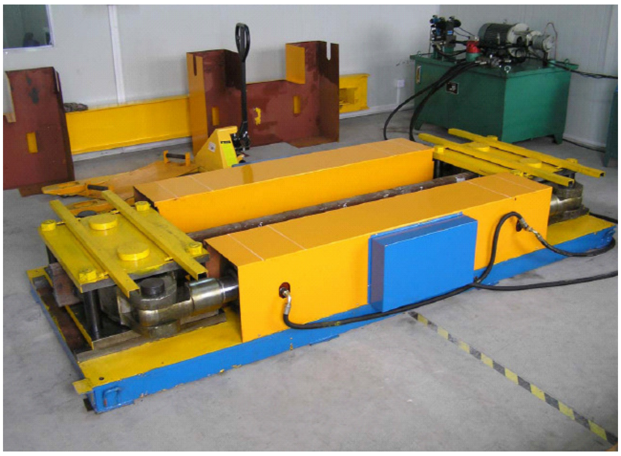

Fig. 12: Calibration test stand designed for the application of high strains.

10. WIDSPREAD USE

The method presented in this article represents a fast measuring method completely non-destructive. Various longitudinal and cross-sectional stress amplitude and distribution measurements are possible. Therewith full-coverage and selective measurements of the neutral temperature are equally possible. Typical applications are:

- general inspections
- prediction and economization of areas to be maintained
- verification and documentation of cw-rail production
- detection of quality and safety endangered locations
- determination of the influence zone length at rail buckles, fractures and in derailment areas
- determination of neutral temperature changes (mobile stress memory unit)

.

SUMMARY

The measurement of the neutral temperature and the longitudinal stress is possible in fixed track between traffic by the help of the presented non-destructive technology. The effectiveness of the technique was significantly increased using a new calibration and measuring procedure. In special areas like inter alia in small curves or misaligned areas the rail stresses may become complex. Catching the relevant stress state in the cw-rail the presented nd- neutral temperature measuring technique enables the assessement of track quality and safety. Also it offers a wide spread use for neutral temperature measurements and covers the actual need of a non-destructive SFT measuring technique.

REFERENCES

/1/ S. Chikazumi, “Physics of magnetism”, John Wiley & Sons, New York 1964

/2/ V. Hauk, „Structural and residual stress analysis by nondestructive methods“, pp. 564-586, Elsevier, ISBN 0-444-82476-6, 1997

/3/ C. Jagadish, L. Clapham, and D. L. Atherton, „Influence of Uniaxial Elastic Stress on Power Spectrum and Pulse Height Distribution of Surface Barkhausen Noise in Pipeline Steel“, IEEE Transactions on magnetics, Vol. 26, No. 3, pp. 1160-1163, 1990

/4/ I. Altpeter, „Spannungsmessung und Zementitgehaltsbestimmung in Eisenwerkstoffen mittels dynamischer magnetischer und magnetoelastischer Messgrößen“, Dissertation Universtät des Saarlandes, unveröffentlicht 1990

/5/ Ch. Baillon, “Soudage SkV-Elite et métrologie des L.R.S.“, Rapport ENSEEG 2ème année, Grenoble, 2006

/6/ Dwight Clark, “Track Buckling Prevention Seminar, AREMA external training course, Charlotte, July 26, 2005